이학석사 학위논문

Reliability study of organic nonvolatile resistive memory at elevated temperatures

온도 상승시 비휘발성 유기 저항 메모리의 소자 안정성에 관한 연구

2016 년 2 월

서울대학교 대학원

물리천문학부

김 영 록

Abstract

In this study, nonvolatile organic memory devices were fabricated by using PI:PCBM (polyimide (PI) and 6-phenyl-C61 butyric acid methyl ester (PCBM) as an active memory material with Al/PI:CPBM/Al structure. As changing temperature from room temperature to 470 K, PI:PCBM organic memory devices showed good nonvolatile memory properties in terms of distribution of ON state current and OFF state current, threshold voltage of OFF state to ON state transition, retention, and endurance. These organic memory devices exhibited excellent ON/OFF ratio ($I_{ON}/I_{OFF} > 10^3$) through more than 200 times ON/Off switching cycles, and maintained ON/OFF states for longer than 10^4 seconds without showing any serious degradation under the measurement temperature up to 470 K. The structural robustness against thermal stress was confirmed through TEM cross-sectional image and AFM image of active layer after retention test at 470 K during 10,000 seconds. This study demonstrated that the operation of organic memory devices under high temperatures was able to be controlled by the parameters which was already used for room temperature, and that the structure of organic memory devices was maintained during thermal stress. These results may make it possible the utility of nonvolatile organic memory devices for high temperature environments.

Keyword : Organic memory, Nonvolatile, PI:PCBM, Thermal stress
Student Number : 2011-20391

Table of Contents

List of Figures

Chapter 1. Introduction

1.1. Achievements of organic memory

In recent decades, to overcome the limitation of inorganic material electronics, organic electronic devices, including organic light-emitting diode, solar cell, sensor, organic field effect transistor and organic memory, have been widely investigated due to their useful properties, such as mechanical flexibility, low cost, large-area fabrication, capability of band gap engineering, simple structure and easy fabrication [1-8]. Among them, organic memory was a one of the promising future data storage devices because of easy of fabrication, clear switching behavior, excellent data keeping property and flexibility [9-11]. Especially, polyimide (PI) block polymer with 6-phenyl-C61 butyric acid methyl ester (PCBM) composite nonvolatile organic resistive memory was one of the strong candidate of flexible memory storage media, because of many of breakthrough for actual application such as micro-scale fabrication, 3-D integration, one transistor - one memory (1T-1R) structure and one diode - one resistor (1D-1R) structure [12-16]. These achievements enhanced integration of PI:PCBM organic memory devices and prevented cross talk problem in organic resistive memory which has cross bar array structure. Those of achievements was based on properties of PI:PCBM organic resistive memory such as simple fabrication process and unipolar resistive memory operation. Although there are progresses of PI:PCBM organic resistive memory, its thermal stability was not explored. Because application of organic electronics is able to be extended to harsh environment such as direct ray of the sun, flexible displays patched on curved surface in outdoor environment and highly integrated electronic circuit which provide high temperatures, verification of thermal robustness of nonvolatile organic memory is significant for its application probability. Many of organic materials such as polystyrene and PMMA, are weak for thermal stress which is able to cause decomposition of organic materials, break bonding between atoms, cause phase transition and transform configuration of organic molecules or macromolecular structures [17-19]. Therefore, the thermal stability of PI:PCBM memory is needed to be explored for its actual application. For PI:PCBM, the memory properties was regarded being induced from PI block and PCBM nanoparticle composite structure. So, PI:PCBM organic memory devices is able to be influenced under high temperature environments through deformation of PI block and any change in composite structure of PI and PCBM.

1.2. Operation under thermal stress

In this study, the electrical thermal stability of PI:PCBM organic resistive memory with glass substrate was confirmed from room temperature to 470 K which was limitation of facilities for electric measurement. Glass substrates were chosen because of its certain thermal robustness. The electric measurement was made up of three parts which were operative characteristics, parameter uniformity and device robustness. Operative characteristic presented behavior of selected one cell of organic resistive memory with temperature elevation. That showed steady current – voltage feature Up to 470 K. From these results I tried to explain the stability of charge transport mechanism. Parameter uniformity means that the one memory operative setting, such as threshold voltage and criteria of ON state and OFF state, was able to be applied for sets of memory cells and for all temperatures. I confirmed parameter uniformity by verifying 32 cells of memory for each temperature. Last, device robustness is consist of retentions test of memory, and endurance tests which are repeated operation test for organic memory devices. Retention and endurance tests exhibited excellent nonvolatile and repeated properties of memory devices from room temperature to 470 K. After retention test at 470 K, the structural maintenance was verified by using transmission electron microscope and atomic force microscope. Through the images of both microscope, I confirmed that the thermal stress did not deform structure of organic memory, and these result supported the electrical stability. This thermal stability demostrates the nonvolatile organic resistive memory as a perspective data storage media.

Chapter 2. Experiments

2.1. Memory material preparation

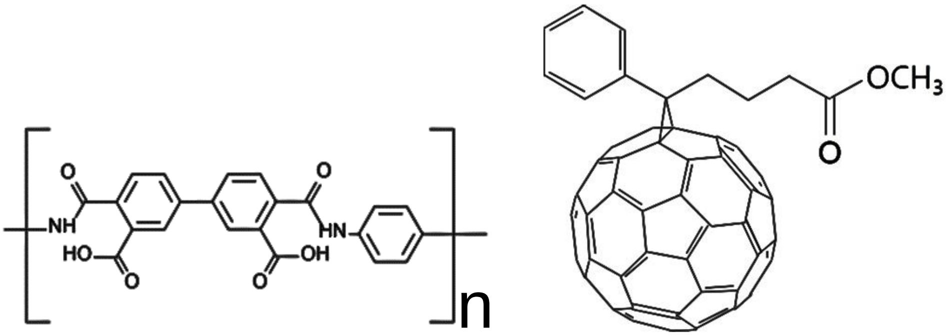

Polyimide(Cured)
BPDA-PPD

PCBM

Fig. 1 Chemical structure of cured PI and PCBM which are used as active memory layer.

Fig. 1 shows the molecular figures of active memory material, PI:PCBM. For this, I prepared the mixture of 3 ml biphenyltetracarboxylic acid dianhydride p-phenylene diamine (BPDA-PPD) solution (10 wt % in N-Methyl-2-pyrrolidone (NMP), purchased from Sigma-Aldrich) as a PI block precursor and 9 ml NMP to optimize solution viscosity. Then I made 0.5 wt % 6-phenyl-C61 butyric acid methyl ester (PCBM, Sigma-Aldrich) solution in NMP. Next, BPDA-PPA and PCBM solution were mixed with volume ratio 1:0.3. Subsequently, the PI:PCBM composite solution was sonicated for 10minute to improve solution uniformity. After that filtered through a 0.20 μm-sized nylon syringe filter to improve surface uniformity of active layer.

2.2. Fabrication

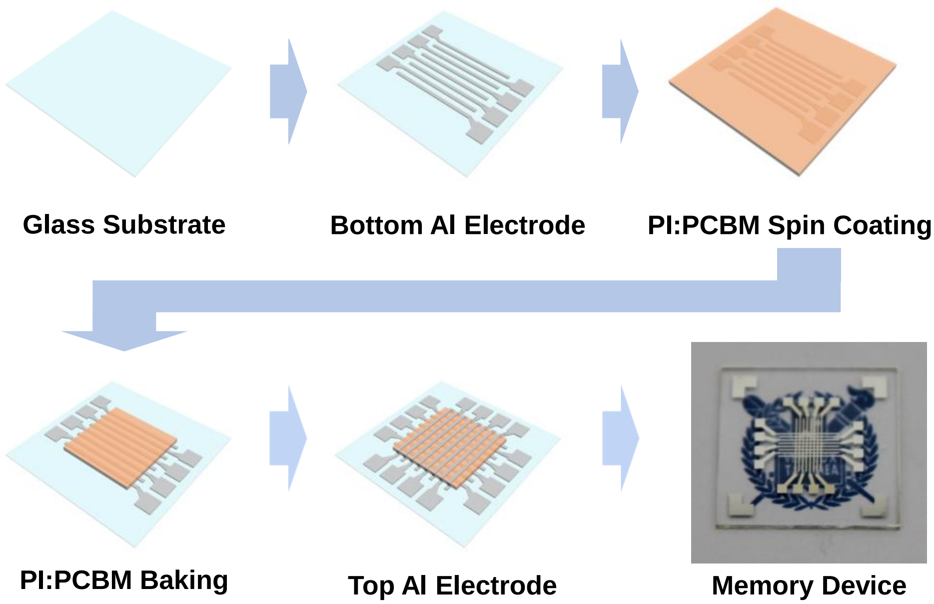

Fig. 2 Schematic illustration of Fabrication process.

Fabrication steps are represented on Fig. 2. In fabrication, first, the glass substrates were cleaned using acetone, isopropanol, and de-ionized water for 10 min at each cleaning solvent under sonication in an ultrasonic bath. After that, the substrates were dried in a vacuum oven at 100 °C for 2 hours to remove residual cleaning solvent on the glass substrates. Next, the 30 nm-thick bottom Al electrodes were deposited on the substrates by thermal evaporator (Korea Vacuum Tech, 15KVS022) using shadow masks with rate 0.5 Å/s under the pressure about 10^{-6} torr. The line width of bottom Al electrodes were 100 µm. Next, bottom Al bottom electrodes and substrates were under UV-ozone treatment to improve uniformity of surface and enhance its memory properties [20-22]. After UV-ozone treatment, active memory layer formation on substrate was done in N_2 filled grove box [12,13,15,23]. The prepared PI:PCBM active layer solution was spin coated on the substrates at 500 rpm 5 s and subsequently 2000 rpm 35 s. Then the substrates were soft baked on a hot plate at 120 °C for 5 min and mopped with swabs soaked in methanol to expose bottom electrodes. Then active memory material was hard baked on the hot plate at 300 ºC for 30 min for block-polymerization of PI. Finally, top Al electrode were deposited as same procedure of bottom electrodes.

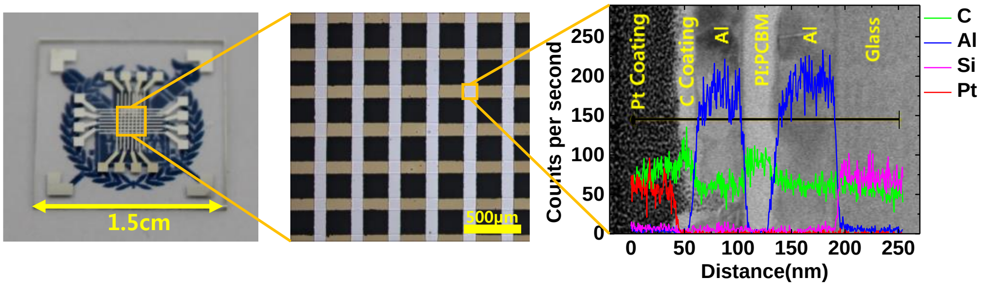

Fig. 3 Optical image and TEM cross sectional image of the fabricated organic memory devices. PI:PCBM layer is about 25 nm-thickness and well separated from both Al electrodes. Energy dispersive X-ray spectroscopy (EDS) data are represented as lines over TEM cross sectional image. Both of TEM cross sectional image and EDS data show clear separation of organic active layer and Al electrodes

The resulting thickness of PI:PCBM layer was about 25 nm by using cross-sectional transmission electron microscopy (TEM) in Fig. 3. The Optical and TEM cross sectional images in Fig. 3 indicates the well-defined PI:PCBM layer (~25nm) between the Al electrodes (~30nm). The energy dispersive X-ray spectroscopy (EDS) data are demonstrated as lines in Fig. 3 over TEM cross sectional image. From EDS data, aluminum was not found in the organic active layer. This result supported distinct separation between organic active layer and Al electrodes. Since the Al penetration in organic layer would create metal filamentary path between top and bottom electrodes and make short circuits in the memory devices, confirmation of absence of Al in memory layer was important to demonstrate the effectiveness of organic memory layer [24]. From the result of EDS data, it were able to be presumed that the nonvolatile memory properties of organic memory devices was caused by characteristic properties of organic memory active layer [25].

2.3. Devices characterization and measurement

The electrical measurement of the memory devices were performed using a semiconductor analyzer system (Model 4200-SCS, Keithley, Inc.) with elevation high temperature from room temperature (300 K) to 470 K under pressure about 10^{-2} mbar in a vacuum probe station with temperature controller (Model ST-500, Janis Research Co.). To make sure the structural robustness of PI:PCBM active layer against thermal stress, both methods, cross section images of memory devices with transmission electron microscope (TEM, JEOL JEM-2100F) and scanned exposed surface of PI:PCBM by atomic force microscope (AFM, Park Systems NX 10 AFM), were performed before and after annealing through retention measurement at 470 K for 10^4 seconds.

Chapter 3. Results and Discussions

3.1. Operation Characteristics

3.1.1. Current-voltage curves

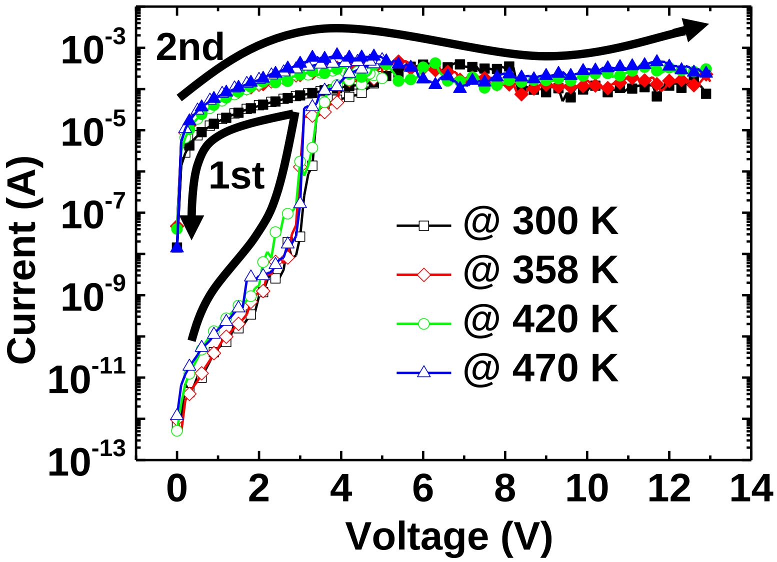

Fig. 4 Current-Voltage (I-V) curves of organic memory devices with temperature variation in same cross point of bottom and top electrodes. I-V curves represent data at 300 K (black), 358 K (red), 420 K (green), and 470 K (blue).

Fig. 4 shows current-voltage (I - V) curves of a selected memory cell with temperature elevation. Here, the bottom electrode were grounded and the external voltage applied to top electrode [26]. Before applied any voltage bias on memory devices, the initial state of the memory cells were in a high-resistive state. At first, on the selected cell, applied voltage was acted on the memory cell from 0 V to 5 V to make low-resistive state from high-resistive state, and then applied voltage 5 V to 0 V to verify that selected memory cell maintained its resistive state without voltage bias acting on. After that, applied voltage was acted on that cell from 0 V to 13 V to verify the nonvolatile property of memory devices. During applying voltage from 0 V to 13 V, the memory cell maintained the low-resistive state, but after 5 V that showed decrease of current level with increasing voltage bias. That phenomenon is called negative differential resistance (NDR). After NDR voltage region, memory cell changed its resistive state from low-resistive state (LRS, ON state) to high-resistive state (HRS, OFF state). So memory device showed resistive state transition after NDR. Since these conductive state change occurred in same voltage bias direction, memory device also exhibited unipolar memory property [21,27]. In all temperatures, the selected memory cell was abruptly changed its resistive state from OFF state to ON state at very similar voltage (about 3 V), when applied voltage bias changed from 0 V to 5 V. Also ON state of the memory cell was retained, when the applied voltage bias changed from 5 V to 0 V at all temperatures. Subsequently, when voltage bias was 0 V to 13 V, all of I - V curves showed nonvolatile memory property from 0 V to 5 V bias region, and also exhibited negative differential resistance (NDR) phenomena about 5 ~ 8 V bias region. After NDR regions, the memory cell changed to OFF state. In Fig. 4, resistive state transition voltages (threshold voltage) and NDR regions ranges were almost same for each temperature. Also the current levels of OFF state and ON state were very similar. So I was able to consider that the threshold voltage and the criteria of ON state and OFF state were invoked commonly to the selected memory cell operation.

3.1.2. ON/OFF current ratios

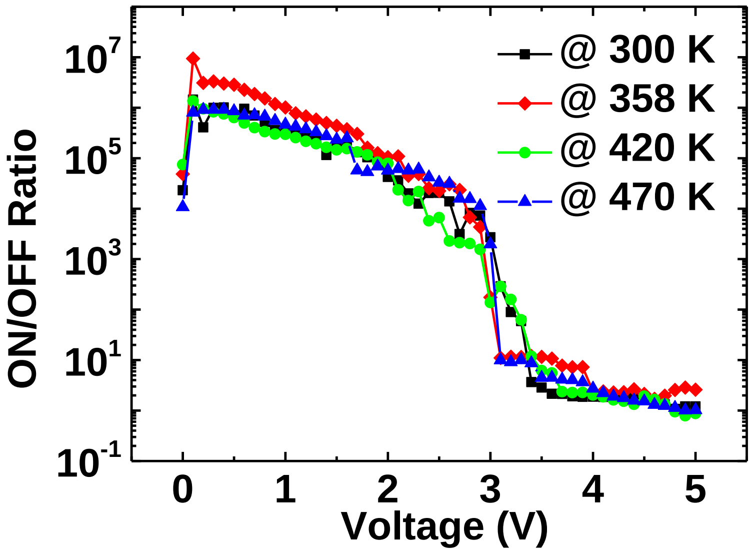

Fig. 5 ON/OFF current ratio of the memory cell versus applied bias for various temperature from fig. 4.

In Fig 5, the ON/OFF ratios of the current level of LRS and that of HRS is represented from bias voltage 0 V to 5 V. Up to 470 K, current ratio curves showed similar features and typical switching property of memory devices, and within 2V memory devices show high ON/OFF ratio (>10^4) for all temperatures. These results represented that the memory devices operated up to 470 K without loss of typical properties of bistable resistivity.

3.1.3. Conducting mechanism

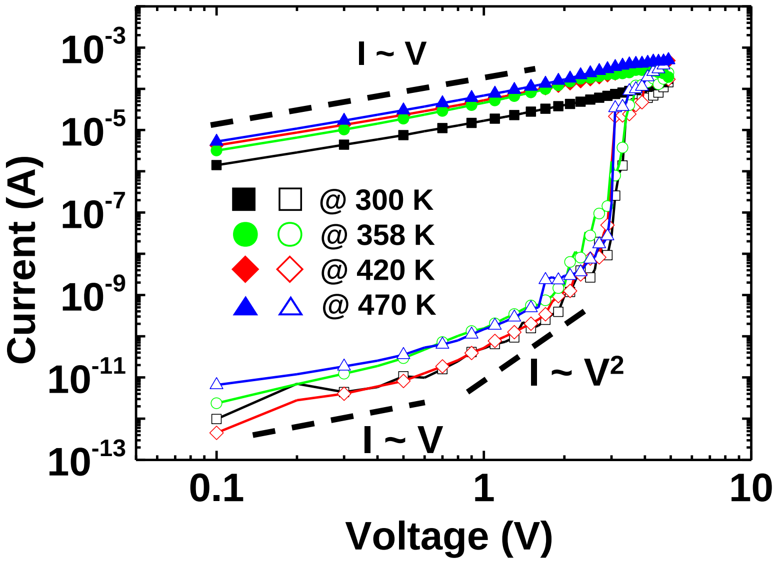

Fig. 6 Logarithmic scales of I-V curves in 0 V ~ 5 V region for each temperature.

For organic resistive memory, these switching phenomena were explained mainly by filamentary conduction mechanism or trap site assisted conduction mechanism [28-31]. Recently, for PI:PCBM nonvolatile resistive organic memory, there was attempt to investigate its conduction mechanism by noise characteristic analysis [25]. In this study, I focused on the conduction characteristics of low voltage region (0 V ~ 5 V) which were actual operating voltage for ON state and OFF state separation. To confirm maintain of charge transporting mechanism, the scales of current and voltage in 0 V ~ 5 V voltage regions of I – V curves in Fig. 5 was converted to logarithmic scales of current and voltage in Fig. 6. Before threshold voltage around 3 V, OFF state curves (empty mark curves) showed almost linear current change to voltage under 1 V, and nearly quadratic variation from 1 V to 2 V for all temperatures. This current tendency was typical space charge limited current (SCLC) curves and I can regard the threshold voltage region as trap charging region of SCLS [32,33]. For ON curve (filled mark curves), I - V curves showed almost linear dependence of current to voltage. So in ON state, current was seem to follows ohmic conductance up to 470 K. For both ON states and OFF states, charge conductance feature were almost unchanged. So I was able to presume that the charge carrier conductance mechanism were maintained under temperature increasing.

3.2. Statistical data under temperature variation

3.2.1. ON current and OFF current statistics

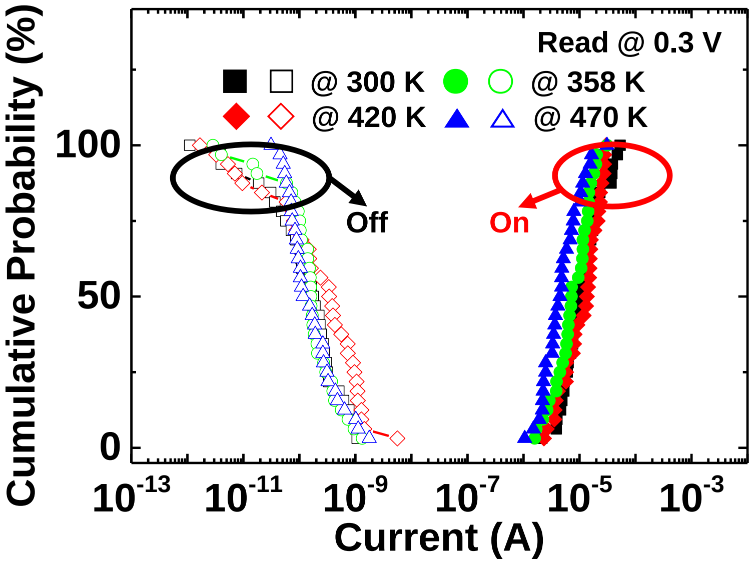

Fig. 7 Cumulative provability of ON and OFF current of 32 cells for each temperature.

Fig. 7 illustrates the statistical data for the switching characteristics of all of the selected memory devices. Before changing temperature from room temperature to 470 K, memory devices were examined to check each devices operate or not. At room temperature, 83 cells out of selected 88 cells operated, so the yield of fabrication is 94.3%. And all of those cells operated for high temperatures. Fig. 7 exhibit the cumulative probability of the ON state current and OFF state currents for all of the operated memory devices at that temperature with read voltage 0.3 V. The distribution of the ON current levels (filled mark curves) were within two order of magnitude, while the OFF current levels (empty mark curves) were in somewhat boarder. However, both ON and OFF current levels were separated more than two order of magnitude from room temperature to 470 K, and I could set distinct criteria for ON and OFF current level. Through results of Fig. 4 and Fig. 7, I verified that the common criteria of ON state current and OFF state current was able to be set not only for one memory cell but also groups of memory cells.

3.2.2. Threshold voltage statistics

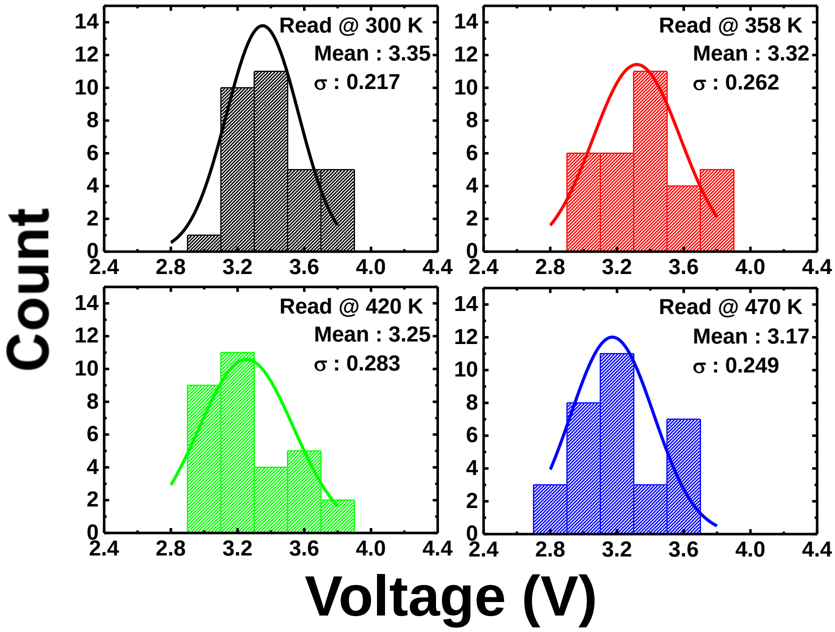

Fig. 8 Distribution of threshold voltages analyzed by Gaussian fitting at each temperature.

Fig. 8 shows statistical data of threshold voltage (V_{th}) of each temperatures. By using Gaussian fitting analysis of each threshold voltage distribution, the standard deviation of threshold voltages were within 0.3 for all temperatures and all the mean values were also near 3.3 V. Therefore, thresghold voltage of organic resistive memory is able to have same value for all temperature. All of detail I- V curves for each temperature are presented following pages.

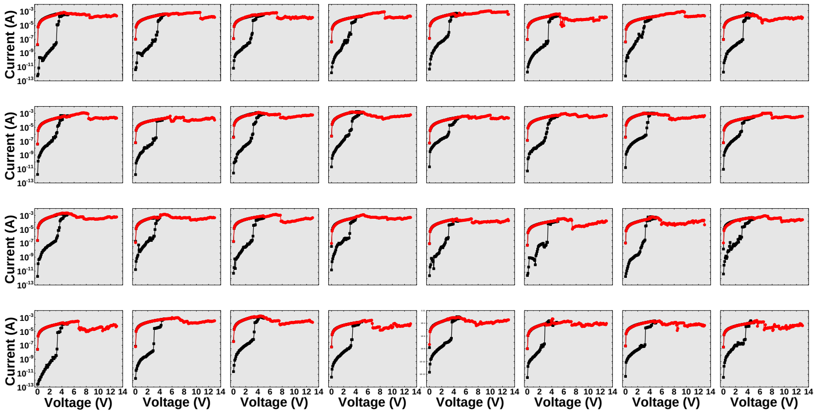

Fig. 9 All of I-V curves which are used in fig. 7 for 300 K.

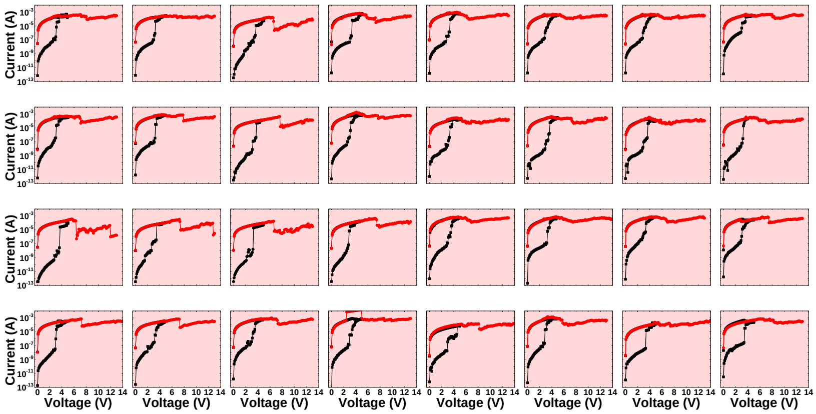

Fig. 10 All of I-V curves which are used in fig. 7 for 358 K.

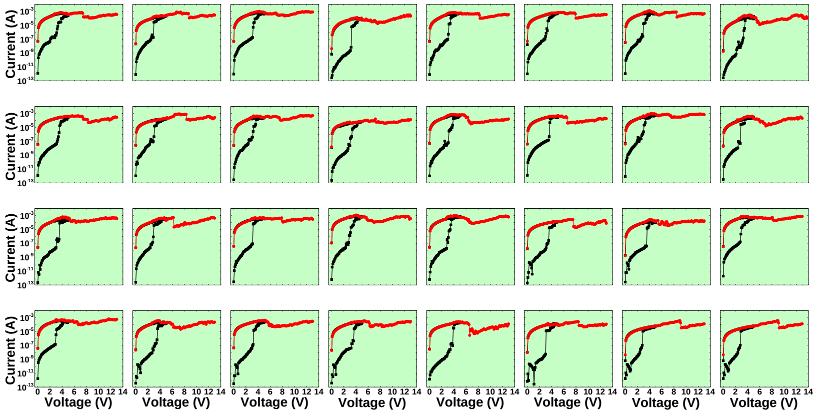

Fig. 11 All of I-V curves which are used in fig. 7 for 420 K.

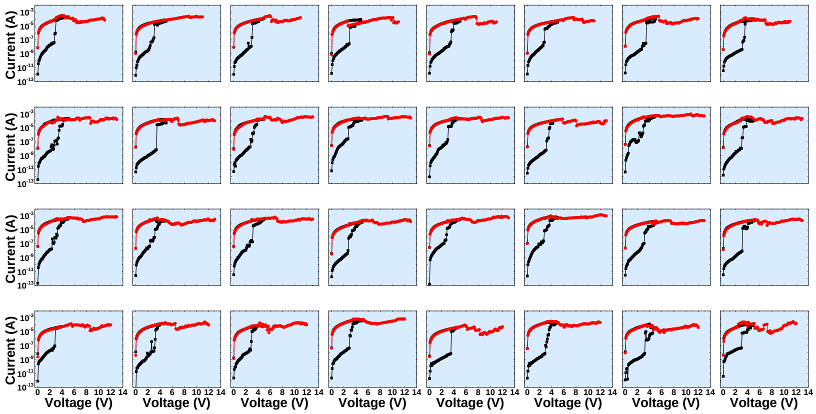

Fig. 12 All of I-V curves which are used in fig. 7 for 470 K.

3.3. Thermal robustness

3.3.1. Electric operation robustness

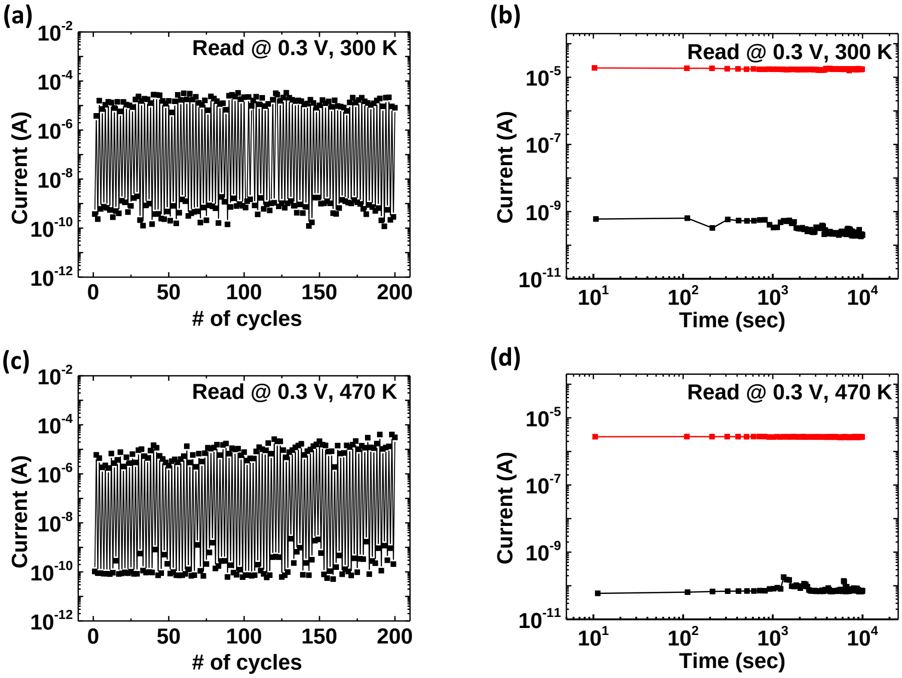

Fig. 13 (a) DC sweep endurance test and (b) retention time test result at 300 K. (c) DC sweep endurance test and (d) retention time test at 470 K.

To verify the memory storage durability and device stability, retention and endurance tests were performed on memory devices. Fig. 13 (a) and (c) shows the DC sweep endurance tests to investigate device switching durability at 300 K and 470 K. I made the memory cell ON state through DC sweep voltage from 0 V to 4 V and decreased applied voltage to 0 V. After that I applied voltage from 0 V to 11 V to change the memory cell to OFF state. These turn on and turn off process repeatedly acted on the memory cells at each temperature to verify the endurance of the memory devices. Currents were read at 0.3 V for each ON and OFF states. Although there were some variations of ON and OFF currents, memory devices held a high ON/OFF ratio over 10^3 during 200 repeated switching cycles for all temperatures. So I was able to regard organic memory devices are stably operating repeatedly up to 470 K. I measured the current level of ON state and OFF state for 10^4 seconds with a measurement interval of 10 seconds at read voltage of 0.3 V to confirm that organic memory device maintained its nonvolatile property for enough long time. Fig. 13 (b) and (d) shows the results of retention test of for 300 K and 470 K. The current level ratios of ON state and OFF state maintained more than 10^3 times without any serious degradation for the both states. The similar results were repeated at 358 K and 420 K. The results at 358 K and 420 K are represented below.

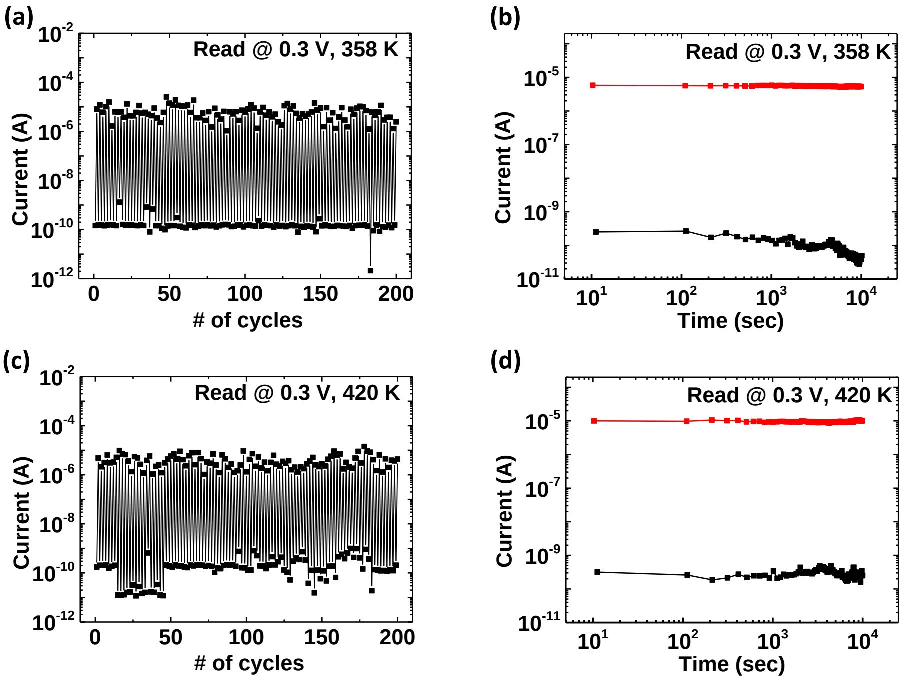

Fig. 14 (a) DC sweep endurance test and (b) retention time test result at 358 K. (c) DC sweep endurance test and (d) retention time test at 420 K.

3.3.2. Structural robustness

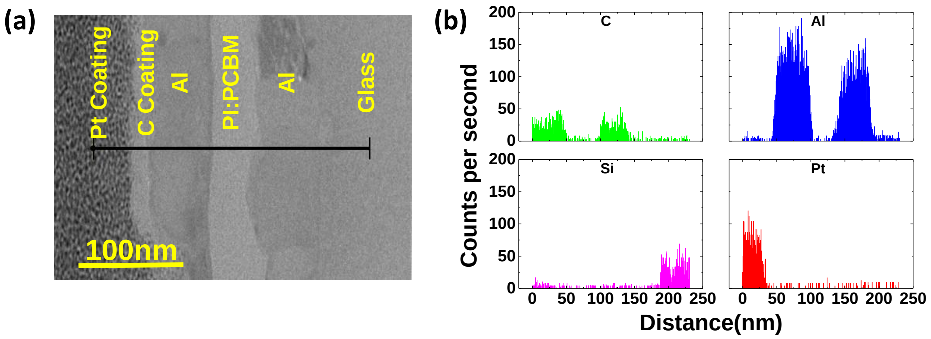

Fig. 15 (a) TEM cross sectional image and (b) EDS data after annealing by retention at 470 K during 10^4 seconds.

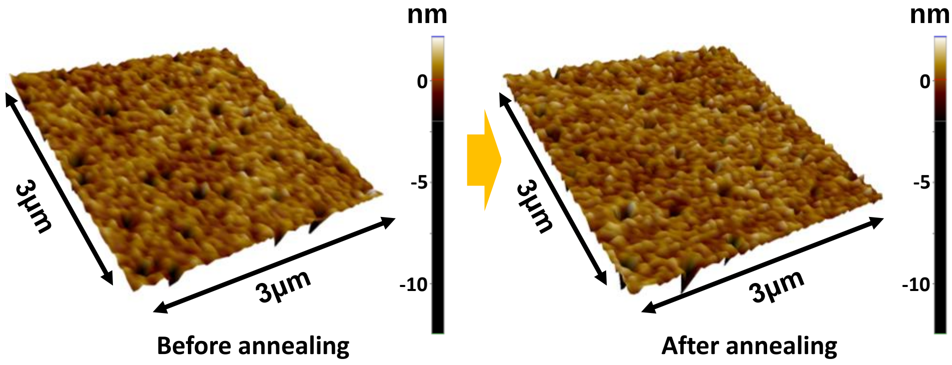

Fig. 16 AFM surface image of exposed PI:PCBM active layer before and after annealing.

Since temperature change and thermal stress were able to cause deformation of the structure of device and atomic composition of the each layer of memory devices, I compare TEM cross sectional images and AFM images of memory devices before and after annealing through retention test at 470 K for 10^4 seconds. Fig. 15 demonstrates the TEM cross sectional image and EDS data after annealing. Comparison between Fig. 3 and Fig. 5 did not show any significant difference between both images. Both of TEM cross sectional images showed about 25nm thickness of active memory layer. EDS data for after annealing test sample exhibited that the elements of each part of memory also does not change. That results implies that in spite of thermal expansion and contraction, and heating during annealing, there were no formation of filamentary path of aluminum, and also no deformation of device structure. These results represent directly that memory devices have structural resistance against thermal stress and that aluminum filamentary path was not formed during heating. I also verified any change of surface through AFM image of exposed PI:PCBM surface on device substrate. Fig. 16 is AFM images of PI:PCBM surfaces before and after annealing. For AFM image of the pristine PI:PCBM sample in Fig. 16, AFM surface images exhibited porous structure on the surfaces of PI:PCBM images. The diameter of the porous structure was about 100 nm to 200 nm. However, the deepest pole had about 10nm which is less than half of PI:PCBM active layer thickness. So the porous structure on PI:PCBM layer did not contribute to conformation of the aluminum filamentary path between top and bottom electrodes which was able to generate short circuits instead of electrical memory behavior. These porous structures seem to be created by evaporation of solvent (NMP) during baking processes [34]. Although change of temperature was able to cause deformation such as clacks on PI:PCBM surface, both of AFM images did not show any significant difference on surfaces, supporting structural robustness against thermal stress on active memory layer.

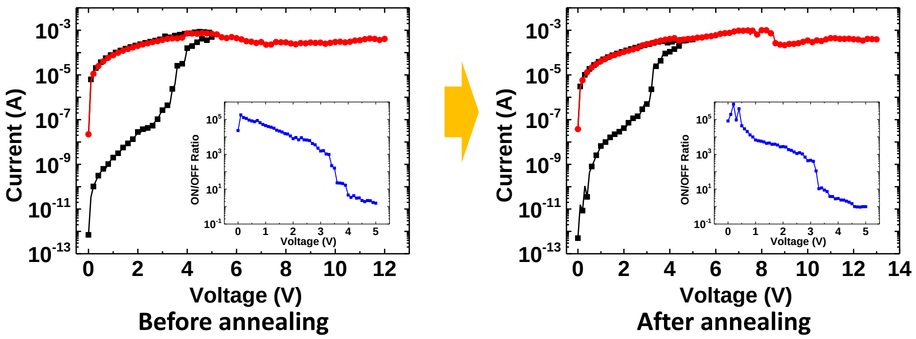

Fig. 17 I-V curves before and after annealing. Insets of both graphs demonstrate ON/OFF current ratios from 0 V ~ 5 V.

After retention test at 470 K, I operated the memory devices again to confirm that device I –V properties also retain after thermal stresses. Fig. 17 shows both of I-V curves before and after annealing, those two curves show very similar feature. Through this result, I was able to verify that electrical properties of organic memory devices also retained for both way of temperature changes up and down from room temperature to 470 K. These electrical and structural thermal robustness are presumed due to thermal stability of polyimide which is organic memory layer block, because transition temperature of polyimide (Sigma-Aldrich) is upper than 400 ^{o}C after imidization. Thermal solidity of structure of organic memory devices were considered as one of the reason of electrical stability under temperature elevation.

Chapter 4. Conclusions

In this study, I verified thermal robustness of PI:PCBM unipolar organic resistive memory through confirmation of its electrical characteristics and structural robustness under high temperature environment. From room temperature to 470 K, organic memory devices I – V curves exhibited stable switching performance such as similar current levels for each measurements, steady ON/Off current ratio and unchanged conductive features which was seem to have ohmic conductance at ON state and SCLS conductance at OFF state. Those results showed that same operative parameters such as turn on voltage and ON and OFF state criteria are able to be used for various temperature from room temperature to 470 K. The cumulative data of many of memory cells showed that the operational parameters such as threshold voltage and ON/OFF state criteria are applied commonly to each of the memory cell at all temperature up to 470 K. The results of the retention and endurance test exhibited that the nonvolatile property of organic memory devices is persistent under high temperature. Also, through TEM cross sectional images and AFM surface images, I verified organic memory device structure was stable under thermal stress. These structural thermal robustness were one of basis of the electric thermal stability of memory devices. This thermal robustness of rganic memory devices promises application of organic flexible electronics for high temperature environments.

Appendix

1. The poster which was presented in ICME&D 2015, Seoul

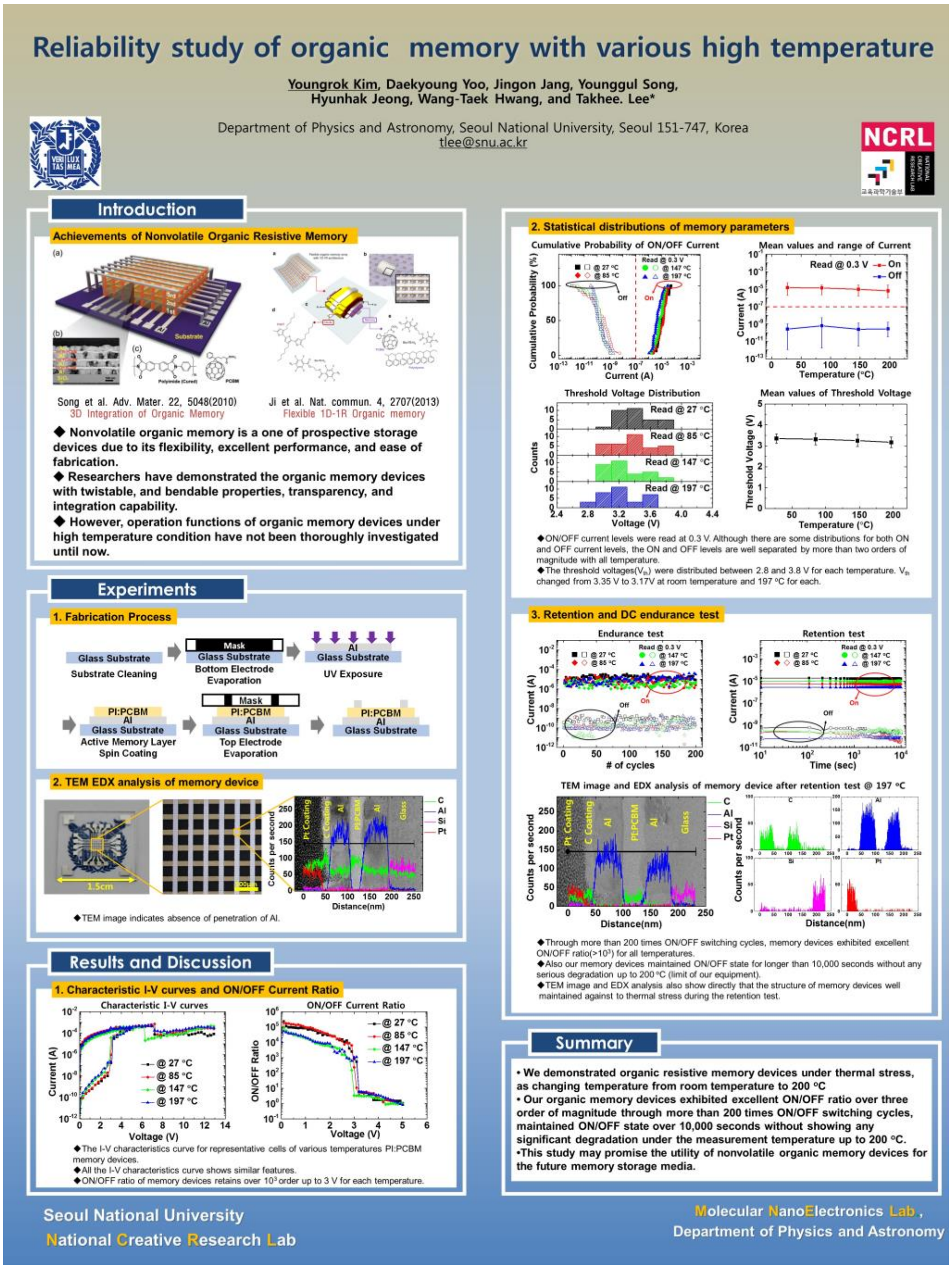

Reliability study of organic memory with various high temperature
Youngrok Kim, Daekyoung Yoo, Jingon Jang, Younggul Song, Hyunhak Jeong, Wang-Taek Hwang, and Takhee. Lee*
Department of Physics and Astronomy, Seoul National University, Seoul 151-747, Korea
tlee@snu.ac.kr
NCRL
Introduction
Achievements of Nonvolatile Organic Resistive Memory
Song et al. Adv. Mater. 22, 5048(2010)
3D Integration of Organic Memory
Ji et al. Nat. commun. 4, 2707(2013)
Flexible 1D-1R Organic memory
◆ Nonvolatile organic memory is a one of prospective storage devices due to its flexibility, excellent performance, and ease of fabrication.
◆ Researchers have demonstrated the organic memory devices with twistable, and bendable properties, transparency, and integration capability.
◆ However, operation functions of organic memory devices under high temperature condition have not been thoroughly investigated until now.
Experiments
1. Fabrication Process
Glass Substrate
Substrate Cleaning
Mask
Glass Substrate
Bottom Electrode Evaporation
Al
Glass Substrate
UV Exposure
PI:PCBM
Al
Glass Substrate
Active Memory Layer Spin Coating
Mask
PI:PCBM
Al
Glass Substrate
Top Electrode Evaporation
PI:PCBM
Al
Glass Substrate
2. TEM EDX analysis of memory device
1.5cm
Pt Coating
C Coating
Al
PI:PCBM
Al
Glass
C
Al
Si
Pt
Counts per second
Distance(nm)
◆TEM image indicates absence of penetration of Al.
Results and Discussion
1. Characteristic I-V curves and ON/OFF Current Ratio
Characteristic I-V curves
Current (A)
Voltage (V)
@ 27 °C
@ 85 °C
@ 147 °C
@ 197 °C
ON/OFF Current Ratio
ON/OFF Ratio
Voltage (V)
◆The I-V characteristics curve for representative cells of various temperatures PI:PCBM memory devices.
◆All the I-V characteristics curve shows similar features.
◆ON/OFF ratio of memory devices retains over 10³ order up to 3 V for each temperature.
2. Statistical distributions of memory parameters
Cumulative Probability of ON/OFF Current
Cumulative Probability (%)
Current (A)
Off
On
Mean values and range of Current
Read @ 0.3 V
On
Off
Current (A)
Temperature (°C)
Threshold Voltage Distribution
Read @ 27 °C
Read @ 85 °C
Read @ 147 °C
Read @ 197 °C
Counts
Voltage (V)
Mean values of Threshold Voltage
Threshold Voltage (V)
Temperature (°C)
◆ON/OFF current levels were read at 0.3 V. Although there are some distributions for both ON and OFF current levels, the ON and OFF levels are well separated by more than two orders of magnitude with all temperature.
◆The threshold voltages(Vth) were distributed between 2.8 and 3.8 V for each temperature. Vth changed from 3.35 V to 3.17V at room temperature and 197 °C for each.
3. Retention and DC endurance test
Endurance test
Read @ 0.3 V
@ 27 °C
@ 85 °C
@ 147 °C
@ 197 °C
Current (A)
# of cycles
On
Off
Retention test
Current (A)
Time (sec)
TEM image and EDX analysis of memory device after retention test @ 197 °C
Pt Coating
C Coating
Al
PI:PCBM
Al
Glass
C
Al
Si
Pt
Counts per second
Distance(nm)
◆Through more than 200 times ON/OFF switching cycles, memory devices exhibited excellent ON/OFF ratio(>10³) for all temperatures.
◆Also our memory devices maintained ON/OFF state for longer than 10,000 seconds without any serious degradation up to 200 °C (limit of our equipment).
◆TEM image and EDX analysis also show directly that the structure of memory devices well maintained against to thermal stress during the retention test.
Summary
• We demonstrated organic resistive memory devices under thermal stress, as changing temperature from room temperature to 200 °C
• Our organic memory devices exhibited excellent ON/OFF ratio over three order of magnitude through more than 200 times ON/OFF switching cycles, maintained ON/OFF state over 10,000 seconds without showing any significant degradation under the measurement temperature up to 200 °C.
•This study may promise the utility of nonvolatile organic memory devices for the future memory storage media.
Seoul National University
National Creative Research Lab
Molecular NanoElectronics Lab ,
Department of Physics and Astronomy

References

[1] A. J. Heeger, S. Kivelson, J. R. Schrieffer, W.-P. Su, Rev. Mod. Phys. 60 (1988) 781.

[2] G. Yu, J. Gao, J. C. Hummelen, F. Wudl, A. J. Heeger, Science 270 (1995) 1789.

[3] S. R. Forrest, Nature 428 (2004) 911.

[4] J. C. Scott, L. D. Bozano, Adv. Mater. 19 (2007) 1452.

[5] J. Rivnay, L. H. Jimison, J. E. Northrup, M. F. Toney, R. Noriega, S. Lu, T. J. Marks, A. Facchetti, A. Salleo, Nat. Mater. 8 (2009) 952.

[6] Y.-Y. Noh, N. Zhao, M. Caironi, H. Sirringhaus, Nat. Nanotechnol. 2 (2007) 784.

[7] H. Yan, Z. Chen, Y. Zheng, C. Newman, J. R. Quinn, F. Dötz, M. Kastler, A. Facchetti, Nature 457 (2009) 679.

[8] T. Sekitani, H. Nakajima, H. Maeda, T. Fukushima, T. Aida, K. Hata, T. Someya, Nat. Mater. 8 (2009) 494.

[9] J. Ouyang, C.-W. Chu, C. R. Szmanda, L. Ma, Y. Yang, Nat. Mater. 3 (2004) 918.

[10] Y. Ji, D. F. Zeigler, D. S. Lee, H. Choi, A. K.-Y. Jen, H. C. Ko, T.-W. Kim, Nat. Commun. 4 (2013) 2707.

[11] L. D. Bozano, B. W. Kean, M. Beinhoff, K. R. Carter, P. M. Rice, J. C. Scott, Adv. Funct. Mater. 15 (2005) 1933.

[12] Y. Song, J. Jang, D. Yoo, S.-H. Jung, S. Hong, J.-K. Lee, T. Lee, Org. Electron. 17 (2015) 192.

[13] D. Yoo, Y. Song, J. Jang, W.-T. Hwang, S.-H. Jung, S. Hong, J.-K. Lee, T. Lee, Org. Electron. 21 (2015) 198.

[14] B. Cho, T.-W. Kim, S. Song, Y. Ji, M. Jo, H. Hwang, G.-Y. Jung, T. Lee, Adv. Mater. 22 (2010) 1228.

[15] S. Song, B. Cho, T.-W. Kim, Y. Ji, M. Jo, G. Wang, M. Choe, Y. H. Kahng, H. Hwang, T. Lee, Adv. Mater. 22 (2010) 5048.

[16] T.-W. Kim, H. Choi, S.-H. Oh, G. Wang, D.-Y. Kim, H. Hwang, T. Lee, Adv. Mater. 24 (2009) 2497.

[17] E. Kiran, J. K. Gillham, J. Appl. Polym. Sci. 20 (1976) 2045.

[18] K. E. J. Barrett, J. Appl. Polym. Sci. 11 (1967) 1617.

[19] S. V. Levchik, E. D. Weil, M. Lewin, Polym. Int. 48 (1999) 532.

[20] B. Cho, S. Song, Y. Ji, T. Lee, Appl. Phys. Lett. 97 (2010) 063305.

[21] F. Verbakel, S. C. J. Meskers, R. A. J. Janssen, H. L. Gomes, M. Cölle, M. Büchel, D. M. de Leeuw, Appl. Phys. Lett. 91 (2007) 192103.

[22] Y. Ji, B. Cho, S. Song, T.-W. Kim, M. Choe, Y. H. Kahng, T. Lee, Adv. Mater. 22 (2010) 3071.

[23] B. Cho, K. H. Nam, S. Song, Y. Ji, G.-Y. Jung, T. Lee, Curr. Appl. Phys. 12 (2012) 940.

[24] B. Cho, J.-M. Yun, S. Song, Y. Ji, D.-Y. Kim, T. Lee, Adv. Funct. Mater. 21 (2011) 3976.

[25] Y. Song, H. Jeong, J. Jang, T.-Y. Kim, D. Yoo, Y. Kim, H. Jeong, T. Lee, ACS Nano 9 (2015) 7697.

[26] B.-G. Kang, J. Jang, Y. Song, M.-J. Kim, T. Lee, J.-S. Lee, Macromolecules 47 (2014) 8625.

[27] J. J. Kim, B. Cho, K. S. Kim, T. Lee, G. Y. Jung, Adv. Mater. 23 (2011) 2104.

[28] L. D. Bozano, B. W. Kean, V. R. Deline, J. R. Salem, J. C. Scott, Appl. Phys. Lett. 84 (2004) 607.

[29] F. Verbakel, S. C. J. Meskers, R. A. J. Janssen, J. Appl. Phys. 102 (2007) 083701.

[30] S. B. Lee, S. Park, J. S. Lee, S. C. Chae, S. H. Chang, M. H. Jung, Y. jo, B. Kahng, B. S. Kang, M.-J. Lee, T. W. Noh, Appl. Phys. Lett. 95 (2009) 122112.

[31] P. R. F. Rocha, H. L. Gomes, L. K. F. Vandamme, Q. Chen, A. Kiazadeh, D. M. de Leeuw, S. C. J. Meskers, IEEE Trans. Electron Devices 59 (2012) 2483.

[32] M. A. Lampert, Phys. Rev. 103 (1956) 1648.

[33] T.-W. Kim, S.-H. Oh, H. Choi, G. Wang, H. Hwang, D.-Y. Kim, T. Lee, Appl. Phys. Lett. 92 (2008) 253308.

[34] J.-C. Chen, C.-L. Liu, Y.-S. Sun, S.-H. Tung, W.-C. Chen, Soft Matter 8 (2012) 526.

국문초록

온도 상승시 비휘발성 유기 저항 메모리의 소자 안정성에 관한 연구

이 연구에서 폴리이미드와 페닐기 뷰트릭 산 메틸 에스터(polyimide (PI) and 6-phenyl-C61 butyric acid methyl ester (PCBM))를 활성 메모리 물질로 사용하여 알루미늄/PI:PCBM/알루미늄 구조를 갖는 비휘발성 유기 메모리를 제작하였다. 온도를 상온에서 470켈빈까지 상승시키면서 ON 상태 전류와 OFF상태 전류 분포, OFF상태에서 ON상태로 전이 문턱전압, 전기전도 상태유지 및 내구성이란 측면에서 메모리소자가 좋은 비휘발성 성질을 갖는다는 것을 보였다. 470켈빈까지 우리의 유기 메모리 소자는 10^3이상의 탁월한 ON/OFF전류비를 보여주었으며 중대한 성능 저하 없이 200회 이상의 ON/OFF상태 전이 와 10^4초 이상의 전기전도 상태유지를 보여주었다. 또한, 470켈빈에서 10^4초 상태유지 시험 후, 우리는 TEM 단층 영상과 AFM표면 영상을 통해 열적 스트레스에 대해서 소자의 구조의 견고함을 확인하였다. 이 연구는 높은 온도에서도 상온에서 정한 작동변수로 유기 메모리 소자를 작동시킬 수 있다는 것을 보여주었다. 이 결과는 고온 환경에서 비휘발성 유기 메모리 소자의 사용을 가능하게 할 것이다.

주요어 : 유기 저항 메모리, 비휘발성, 폴리이미드 피씨비엠, 열적 스트레스

학번 : 2011-20391